Article

Critical Shear Rate of Polymer-Enhanced Hydraulic Fluids

Pawan Panwar [1], Paul Michael [2], Mark Devlin [3] and Ashlie Martini [1]*

[1] Department of Mechanical Engineering, University of California Merced
[2] Fluid Power Institute, Milwaukee School of Engineering
[3] Afton Chemical, Richmond, VA
* Correspondence: amartini@ucmerced.edu

Version October 23, 2022 submitted to Lubricants

Supplemental Information

S1. Instruments

A Cannon StressTech HR Oscillatory Rheometer was used to measure dynamic viscosity at low shear rates and the PCS Ultra Shear viscometer was used to measure the dynamic viscosity at high shear conditions. Schematics of these devices are shown in Fig. S1.

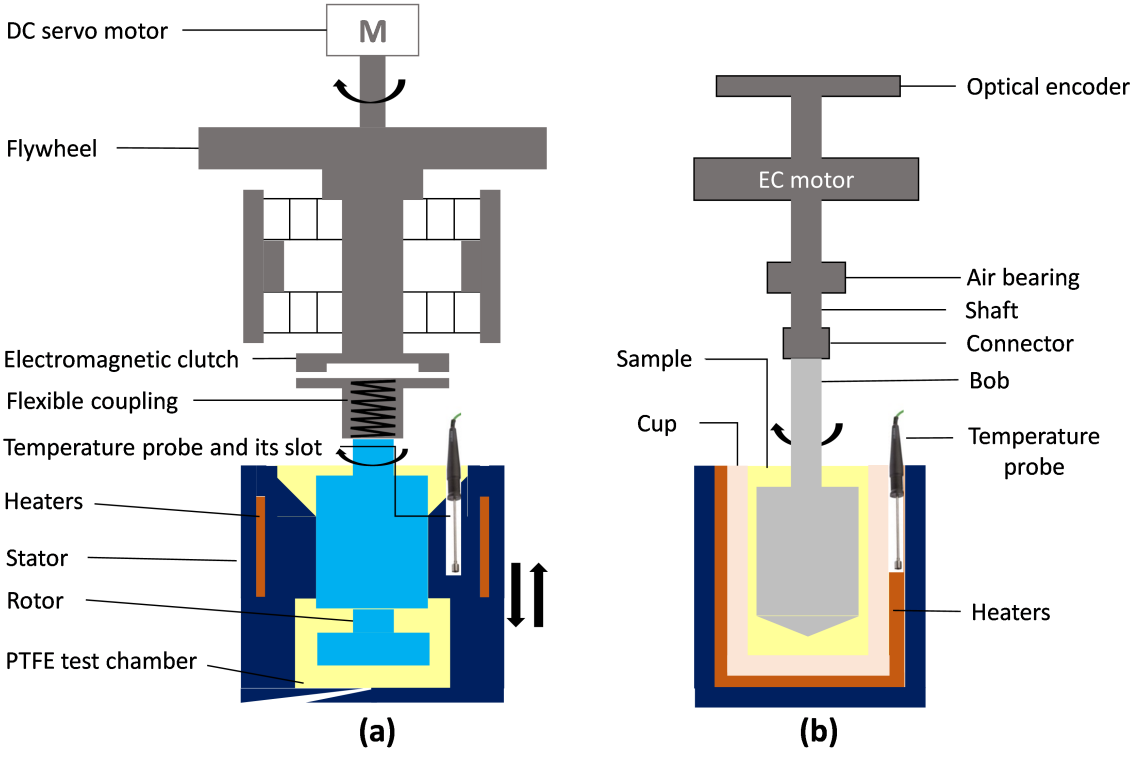

Figure S1. Schematics of (a) PCS Ultra Shear Viscometer and (b) Cannon StressTech HR Oscillatory Rheometer used for measuring high and low shear viscosity, respectively.

S2. Force Field Parameters

The TraPPE-UA forcefield was used to describe the chemistry of molecules. In the TraPPE-UA force field, the nonbonded interactions are described by pairwise-additive Lennard-Jones 12-6 potentials, electrostatic interactions by the Ewald summation, bonded atoms are considered to have

fixed bond lengths, bond angles are governed by harmonic potential, and the motion of the dihedral angle is governed by Fourier potential. The original TraPPE uses fixed bond lengths, but to model fully flexible bonds, a harmonic potential was implemented by taking the corresponding force constants from the CHARMM [1,2] force field, as suggested by Siepmann [3]. This fully flexible model can be described by Equation S.1.

$$\begin{aligned} U_{total} &= U_{bond}(r) + U_{bend}(\theta) + U_{torsion}(\phi) + U_{NB}(r_{ij}) \\ &= \sum_{bond} \frac{k_l}{2}(r - r_0)^2 + \sum_{bend} \frac{k_\theta}{2}(\theta - \theta_{eqm})^2 + \sum_{torsion} \sum_{i=1}^{m} c_i[1 + \cos(n_i\phi - d_i)] \\ &\quad + \sum_{i<j} 4\epsilon_{ij}\left[\left(\frac{\sigma_{ij}}{r_{ij}}\right)^{12} - \left(\frac{\sigma_{ij}}{r_{ij}}\right)^{6}\right] + \frac{q_i q_j}{4\pi\epsilon_0 r_{ij}} \end{aligned} \tag{S.1}$$

Here, r is the bond length, r_0 is the equilibrium bond length, k_l is the bond length force constant, θ is the bond angle, θ_{eq} is the equilibrium bond angle, k_θ is the bond angle force constant, r_{ij} is the site-site separation, ϵ_{ij} is the LJ well depth and diameter and q_i and q_j are the partial charges on sites i and j, respectively. For LJ interactions between two different atom types, the standard Lorentz-Bethelot empirical combining rules were used to compute parameters using Equation S.2.

$$\sigma_{ij} = \frac{1}{2}\left(\sigma_{ii} + \sigma_{jj}\right) \quad \epsilon_{ij} = \left(\epsilon_{ii}\epsilon_{jj}\right)^{1/2} \tag{S.2}$$

For the saturated and unsaturated hydrocarbons, all pseudo-atoms were connected to pseudo-atoms formed from heavy atoms of the same electronegativity; thus, partial charges are not needed here for the TraPPE-UA potential.

The potential parameters that are used to fully describe these molecules are given in Tables S1, S2, S3, and S4.

Table S1. UA force field parameters for non-bonded interactions [3–5].

Pseudo/United atom	ϵ/k_B [K]	σ [Å]	q [e]
CH_3 (sp^3)	98.0	3.750	0.0
CH_2 (sp^3)	46.0	3.950	0.0
CH_2 (sp^2)	85.0	3.675	0.0
CH (sp^3)	10.0	4.680	0.0
C (sp^3)	0.5	6.400	0.0
C (sp^2)	20.0	3.850	0.0

Table S2. UA force field parameters for 1-2 bonded interactions [1–6].

Bond	r_0 [Å]	k_l/k_B [K/Å^2]
CH_x-CH_y	1.54	452900
CH_x=CH_y	1.33	825280

Table S3. UA force field parameters for 1-3 bonded interactions [3–5].

Bond	θ_0 [Å]	k_θ/k_B [K/rad^2]
CH_x-CH_2-CH_y	114.0	62500
CH_x-CH-CH_y	112.0	62500
CH_x-C-CH_y	109.5	62500
CH_x=C-CH_y	119.7	70420

Table S4. UA force field parameters for 1-4 bonded interactions [3–5].

Bond	c_0/k_B [K]	c_1/k_B [K]	c_2/k_B [K]	c_3/k_B [K]
CH_x-CH_2-CH_2-CH_y	0.00	355.03	-68.19	791.32
CH_x-CH_2-CH-CH_y	-251.06	428.73	-111.85	441.27
CH_x-CH_2-C-CH_y	0.00	0.00	0.00	461.29
CH_x-CH_2-C=CH_y	688.50	86.36	-109.77	-282.24

S3. Viscosity Simulation Details

The low-shear or Newtonian viscosity of fluids was modeled using the GreenKubo (GK) approach which relate the shear viscosity to the integral over time of the pressure tensor autocorrelation function [7,8]

$$\eta_0 = \frac{V}{k_B T} \int_0^\infty <P_{\alpha\beta}(t) P_{\alpha\beta}(0)> \mathrm{d}t \tag{S.3}$$

Here, V is the system volume, k_B is the Boltzmann constant, T is the temperature, $P_{\alpha\beta}$ denotes the element $\alpha\beta$ of the pressure or stress tensor, and the angle bracket indicates the ensemble average.

The high shear viscosity η in the non-equilibrium molecular dynamics simulation was determined by computed the ratio of shear stress P_{xz} to the shear rate $\dot{\gamma}$.

$$\eta = -\frac{P_{xz}}{\dot{\gamma}} \tag{S.4}$$

S4. Governing Equations

Rouse Model: The Rouse model [9–11] provides the relaxation times as a function of density ρ and viscosity η_0 of fluid, and the molecular weight M of polymer as

$$1/\lambda = \frac{\pi^2}{12} \frac{\rho R_g T}{\eta_0 M} \tag{S.5}$$

Bird et al. Model: This model [12,13] provides the relaxation times as a function of density ρ and viscosity η_0 of fluid, and the molecular weight M and concentration c_p of polymer. In addition to this, it consider the viscosity η_{0s} of solvent which is base oil in this case.

$$1/\lambda = \frac{c_p \rho R_g T}{(\eta_0 - \eta_{0s}) M} \tag{S.6}$$

Kendall-Monroe: The kinematic viscosity of blend of polymer and base oil was determined by the Kendall-Monroe equation which calculate the viscosity of a blend as the cubic-root average of the viscosity of its components,

$$\mu^{1/3} = x_p \mu_p^{1/3} + x_s \mu_s^{1/3} \tag{S.7}$$

Here, μ, μ_p, and μ_s are the kinematic viscosity of blend, polymer, and base oil or solvent, x_p and x_s are the mole fraction of polymer and base oil in he blend, respectively.

William–Landel–Ferry (WLF): The Newtonian viscosity of polyisobutylene (PIB) as a function of its molecular weight was calculated using an empirical model. This empirical model has been extracted from a large set of experimental data to provide viscosity in mPa·s at 25°C [14,15].

$$\eta_{0p} = 4.69 \times 10^{-9} M^{3.43} \tag{S.8}$$

The viscosity of PIB at any temperature T can be obtained by a temperature shift factor which is described by the WLF equation as

$$\log(a_T) = \log(\eta_{0p}(T)/\eta_{0p}(T_0)) = -\frac{c_1(T-T_0)}{c_2+(T-T_0)} \tag{S.9}$$

Here, T_0 is the reference temperature of 25°C and empirical parameters $c_1 = 8.61$ and $c_2 = 200$ K [14,15].

S5. Carreau Model

Parameter of the Carreau fit to experiment and simulation viscosity data are tabulated in Table S5.

Table S5. Parameter of the Carreau fit to experiment and simulation viscosity data.

Temperature	Fluid ID	Parameters			
		η_0 [mPa·s]	η_∞ [mPa·s]	$\lambda[s]$	n [-]
50°C	Fluid 1	40.149	0.000	1.898×10^{-6}	0.763
	Fluid 2	61.917	1.564	3.592×10^{-6}	0.712
	Fluid 3	35.451	0.000	3.693×10^{-8}	0.671
80°C	Fluid 1	15.837	0.000	4.143×10^{-7}	0.793
	Fluid 2	22.260	0.000	7.742×10^{-7}	0.790
	Fluid 3	13.483	0.000	9.932×10^{-9}	0.662

References

1. Vanommeslaeghe, K.; Hatcher, E.; Acharya, C.; Kundu, S.; Zhong, S.; Shim, J.; Darian, E.; Guvench, O.; Lopes, P.; Vorobyov, I.; others. CHARMM general force field: A force field for drug-like molecules compatible with the CHARMM all-atom additive biological force fields. *J. Comput. Chem.* **2010**, *31*, 671–690.
2. Reiher III, W. Theoretical studies of hydrogen bonding. *Ph. D. Thesis at Harvard University* **1985**.
3. Martin, M.G.; Siepmann, J.I. Transferable potentials for phase equilibria. 1. United-atom description of n-alkanes. *J. Phys. Chem. B* **1998**, *102*, 2569–2577.
4. Martin, M.G.; Siepmann, J.I. Novel configurational-bias Monte Carlo method for branched molecules. Transferable potentials for phase equilibria. 2. United-atom description of branched alkanes. *J. Phys. Chem. B* **1999**, *103*, 4508–4517.
5. Wick, C.D.; Martin, M.G.; Siepmann, J.I. Transferable potentials for phase equilibria. 4. United-atom description of linear and branched alkenes and alkylbenzenes. *J. Phys. Chem. B* **2000**, *104*, 8008–8016.
6. Dinpajooh, M.; Nitzan, A. Heat conduction in polymer chains with controlled end-to-end distance. *J. Chem. Phys.* **2020**, *153*, 164903.
7. Zhang, Y.; Otani, A.; Maginn, E.J. Reliable viscosity calculation from equilibrium molecular dynamics simulations: a time decomposition method. *J. Chem. Theory Comput.* **2015**, *11*, 3537–3546.
8. Maginn, E.J.; Messerly, R.A.; Carlson, D.J.; Roe, D.R.; Elliott, J.R. Best practices for computing transport properties 1. self-diffusivity and viscosity from equilibrium molecular dynamics [article v1. 0]. *Living J. Comput. Mol. Sci* **2019**, *1*, 1–20.
9. Rouse Jr, P.; Sittel, K. Viscoelastic properties of dilute polymer solutions. *J. Appl. Phys.* **1953**, *24*, 690–696.
10. Mondello, M.; Grest, G.S.; Webb III, E.B.; Peczak, P. Dynamics of n-alkanes: Comparison to Rouse model. *J. Chem. Phys.* **1998**, *109*, 798–805.
11. Bair, S.; Winer, W.O. A quantitative test of the Einstein–Debye relation using the shear dependence of viscosity for low molecular weight liquids. *Tribol. Lett.* **2007**, *26*, 223.
12. Bird, R.B.; Curtiss, C.F.; Armstrong, R.C.; Hassager, O. *Dynamics of Polymeric Liquids, Volume 2: Kinetic Theory*; Wiley, 1987.
13. Bair, S.S. *High Pressure Rheology for Quantitative Elastohydrodynamics*; Elsevier, 2019.
14. Ferry, J.D. *Viscoelastic properties of polymers*; John Wiley & Sons, 1980.
15. Fetters, L.J.; Graessley, W.; Kiss, A. Viscoelastic properties of polyisobutylene melts. *Macromolecules* **1991**, *24*, 3136–3141.